metals

MDPI

Article

A New Wear Calculation Method for Galvanized Ultra-High-Strength Steel during Hot Stamping

Yuchun Peng [1,2], Wei Chen [1,*] and Hongming Zhou [2]

[1] School of Mechanical Engineering, Jiangsu University, Zhenjiang 212013, China
[2] School of Mechanical and Electrical Engineering, Wenzhou University, Wenzhou 325035, China
* Correspondence: chen_wei@ujs.edu.cn

Abstract: In the hot stamping process, the friction and wear interaction between the high-temperature sheet metal and the water-cooled die has a significant impact on the final quality of the product and the durability of the die. Currently, most research on the wear of the stamped parts during the hot stamping process mainly involves analyzing the wear morphology and wear mechanism of the sheet surface, and there is little research on its wear assessment. In this study, to better assess the forming quality of hot stamping parts, the research takes the direct hot stamping of galvanized ultra-high-strength steel sheets as the object and proposes a wear amount calculation method of galvanized ultra-high-strength steel sheets based on the real contact area of the high-temperature sheet metal and the water-cooled tools. At different temperature conditions, the galvanized layer and steel substrate have different mechanical properties. The model is validated using the sheet characteristics at 650 °C, 700 °C, and 750 °C. The results indicate that the model can predict the wear of the galvanized steel sheet under different conditions within a certain range.

Keywords: hot stamping; ultra-high-strength steel sheet; galvanized layer; wear calculation method

Citation: Peng, Y.; Chen, W.; Zhou, H. A New Wear Calculation Method for Galvanized Ultra-High-Strength Steel during Hot Stamping. *Metals* **2024**, *14*, 756. https://doi.org/10.3390/met14070756

Academic Editor: Bernd-Arno Behrens

Received: 20 May 2024
Revised: 19 June 2024
Accepted: 22 June 2024
Published: 26 June 2024

1. Introduction

With increasing demands on safety, energy conservation, environmental protection, and corrosion resistance in the automotive industry, there are higher requirements for the formability, weldability, surface morphology, painting and corrosion resistance of automotive steels [1–3]. Due to its excellent strength-to-weight ratio and corrosion resistance, ultra-high-strength boron steel sheets are commonly used in the production of automotive A and B pillars and other structural components [4–8]. Galvanized (GA) steel sheet is widely used due to its good corrosion resistance and electrode protection. During the hot stamping process, the significant difference in temperature and hardness between GA ultra-high-strength boron steel sheet and water-cooled dies can easily cause abrasion on the surface of the sheet metal. The surface damage caused by the stamping of GA ultra-high-strength boron steel sheets not only reduces the surface quality of the workpiece and affects its coating performance, leading to decreased corrosion resistance of the workpiece, it also worsens the friction conditions between the high-temperature sheet metal and the water-cooled die contact surface, exacerbating their wear, increasing the cost of die maintenance, and reducing the life span and production efficiency of the die [9,10]. To ensure the forming quality of hot stamping, comprehensive metallurgical evaluations are required for specimen parts. Currently, samples are mainly tested from both micro and macro perspectives to ensure their performance. Common tests include checking whether the macro and micro hardness of the sheet meets the requirements, whether the microstructure reaches a martensitic structure, whether the galvanized layer is intact and properly alloyed, and whether the tensile test meets the requirements.

In recent years, the wear phenomenon of the sheet metal and die during the hot stamping process has attracted the attention of numerous scholars both domestically and

internationally. The wear of GA high-strength steel sheets during hot stamping primarily focuses on the wear mechanism. Ghiotti et al. [11,12] have researched the tribological behavior of hot stamping zinc-coated high-strength steels. Their findings revealed that the chemical diffusion of iron in Zn begins at 700 °C and changes the coating's surface roughness with increasing temperature, which is an evolution of surface morphology related to Zn's boiling point. Compared to the standard Al–Si coating, the higher the sliding speed, the lower the friction of the zinc coating. Hardell et al. [13,14] studied the friction wear behavior of zinc-coated ultra-high-strength steels and die steels under dry friction conditions. They discovered that with increasing temperature and contact pressure, the average friction coefficient showed a decreasing trend, and the zinc coating on the boron steel surface had a more obvious anti-wear effect than nitriding on the tool surface. Kondratiuk et al. [15] conducted a meticulous investigation into the tribological properties of hot dip aluminium-silicon (Al-Si) and electro-plated zinc-nickel (Zn-Ni) alloy coatings, employing hot strip drawing experiments as their methodological approach. Their findings revealed that the Al-Si coating, post-heat treatment, exhibited a distinct tribological behavior compared to the Zn-Ni coating.

Compared with hot stamping, there is relatively more research on the wear of sheet metal in ordinary stamping. Patrik Schwingenschlögl et al. [16] analyzed the friction and wear between die steel and Al–Si coated boron steel sheets during the direct hot stamping process at different temperatures, relative speeds, and contact pressures and detailed the critical relationship between process parameters and tribological behavior. Through tensile tests under hot stamping conditions, they analyzed the friction behavior during the experimental process and measured the wear amount before and after the experiment with a confocal microscope. Wang et al. [17], to clarify the dynamic evolution of the wear initiation of advanced high-strength steel sheets, simulated the sliding test of hot-dip galvanized AHSS sheets on cold-worked DC53 dies using a custom-developed sheet/strip friction tester and discussed the friction behavior and wear mechanisms that influence wear initiation. Zhou et al. [18] revealed the correlation between the plastic deformation level of sheet metal and die surface abrasion. For sheet metal, as plastic deformation increases, the galvanized surface tends to become rough and form a considerable amount of intermittent micro-cracks, leading to early wear initiation. Gao et al. [19] studied the impact of different wear surface morphologies of galvanized automotive steels on stick–slip friction. Their results contribute to a deeper understanding of the mechanism of stick–slip friction of surface wear materials and provide a method to suppress the noise and vibration caused by the stick–slip friction of galvanized automotive steels. Zhuang et al. [20,21] studied the impact of forming damage on the performance of quenched 22MnB5 steel and proposed a damage coupling pre-forming constitutive model for quenched 22MnB5 steel. Through U-shape forming tests, studied the evolution of the surface morphology of hot-dip galvanized (GI) and galvannealed (GA) steels and the impact of die hardness on sheet metal forming (SMF). Results indicate that the surface roughness values of both types of galvanized steel sheets increase with the number of forming operations, and GI steel exhibits better resistance to damage than GA steel. Venema et al. [22] studied the friction and wear mechanisms occurring in thermal friction tensile tests between die steel and Al–Si coated steel sheets at 700 °C, showing that the wear material from the tools could embed into the relatively softer, thin coating. Yu et al. [23] investigated the surface damage behavior of different galvanized steel sheets under bending conditions. The experimental results show that HDGI steel exhibits better damage resistance in metal sheet forming than HDGA steel. In forming HDGI steel, scratches are the primary surface damage, whereas coating peeling and scratches are the two types of surface damage for HDGA steel.

In summary, due to the significant temperature and hardness difference between the high-temperature sheet metal and water-cooled dies and the presence of a galvanized layer, the localized wear mechanism of the sheet metal becomes complex. Current research on the wear of component surfaces is mainly focused on wear mechanisms, with relatively less investigation into the quantitative assessment of component surface wear. However,

in the field of materials science and tribology, the accurate prediction of wear during the hot stamping process is imperative for enhancing the durability of tools and the quality of the stamped components. In this study, we introduce a novel method for calculating sheet wear, which is specifically tailored for the sliding wear occurring on the surface of galvanized ultra-high-strength boron steel sheets during the hot stamping process. This method is predicated on the actual contact area that is present during the frictional process. Utilizing a custom differential temperature friction wear experimental apparatus, we have developed this approach to enhance the accuracy and applicability of wear calculations in this specialized manufacturing scenario. This approach provides a novel perspective for the wear assessment of formed parts.

2. Contact Analysis

During the hot stamping process, the interaction between the die and the sheet metal is pivotal to process efficiency and product quality. The temperature disparity between the water-cooled die and the high-temperature sheet metal creates a contact scenario that can be characterized as a rigid plane (die) engaging with a plastic plane (sheet metal), as visualized in Figure 1. This conceptualization is fundamental to understanding the wear behavior of the sheet metal during the stamping process.

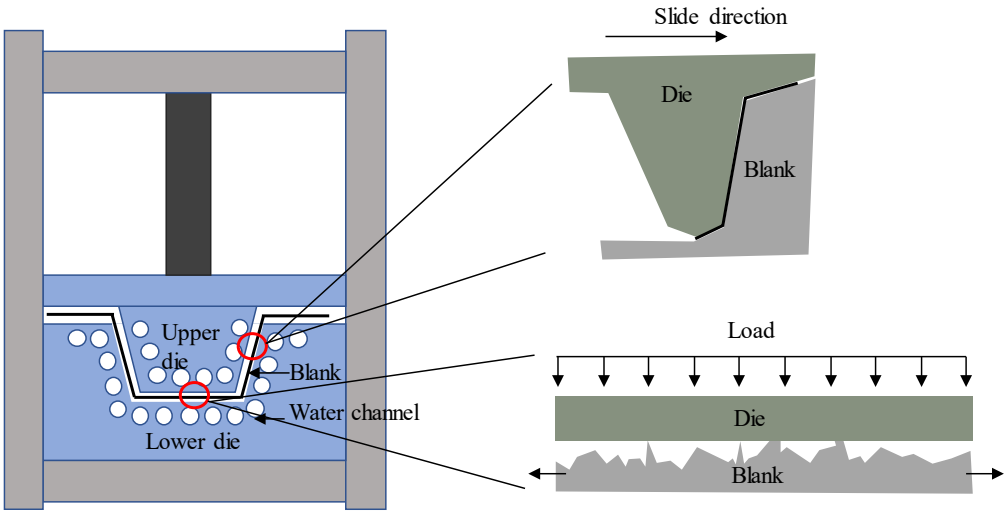

Figure 1. Micro contact diagram between the die and the surface of the sheet metal.

The wear of the sheet metal is predominantly dictated by the real contact area, which is influenced by the material properties and the process conditions [24]. To accurately capture this, a multi-scale contact model is employed, providing a detailed account of the contact dynamics between the die and the sheet metal. This model is instrumental in delineating the real contact area, a critical parameter for wear analysis. Building upon the insights from the multi-scale contact model, a novel calculation method for sliding wear on galvanized ultra-high-strength steel sheets is introduced.

According to pertinent research, it has been established that for hot-formed sheet metal during the forming process, equations representing force balance, energy balance, and volume balance can be formulated [25–27] (Equations (1)–(3)). When these equations are integrated with the specific parameters associated with galvanized boron steel sheet materials [28–33], it becomes feasible to compute the real contact area, denoted as Ar. This calculation is achieved by normalizing the micro-asperities present on the surface of the sheet metal, thereby enabling the determination of the real contact area under various wear conditions.

(1) In accordance with the principle of energy conservation, it is understood that the total internal energy of the sheet metal during the compression phase is equivalent to the external work exerted upon it. This relationship is encapsulated in Equation (1) as follows:

$$W_{ext} = W_{int,ab} + W_{int,sh} \quad (1)$$

where W_{ext} (Nmm) is the external work conducted during the compression of the sheet metal, $W_{int,ab}$ (Nmm) is the energy absorbed by the plastic deformation of the micro-asperities on the surface of the galvanized layer, and $W_{int,sh}$ (Nmm) is the energy required for shear during the relative motion of the micro-asperities on the galvanized layer surface.

(2) During the contact process of the sheet metal, the total normal force is constituted by the following two components: the aggregate normal forces exerted by the contact micro-asperities and the shearing force that arises between the contacting and non-contacting micro-asperities. This comprehensive force relationship is articulated in Equation (2).

$$F_N = F_{c,n} + F_{c,sh} \quad (2)$$

where F_N (N) is the total normal force, $F_{c,n}$ (N) is the normal force of the galvanized contact micro-asperities, and $F_{c,sh}$ (N) is the shearing force between the contacting and non-contacting micro-asperities.

(3) Together, the galvanized layer and the substrate must adhere to the principle of volume conservation throughout the contact phase. This stipulation ensures that the combined volume of these two components remains invariant during the interaction.

$$\Delta V = \Delta V_1 + \Delta V_2 \quad (3)$$

where ΔV is the volume of compressed sheet metal, ΔV_1 is the volume of the compressed galvanized layer, and ΔV_2 is the volume of compressed sheet metal substrate.

The method is anchored in the renowned Greenwood and Williamson (GW) contact model in the field of tribology, which has been extensively validated for its ability to characterize the contact between rough surfaces. The GW model postulates that surface micro-asperities can be idealized as a distribution of hemispheres of varying sizes, which is a critical assumption for understanding the contact mechanics at the micro-scale [34]. As illustrated in Figure 2, this conceptualization provides a clear and concise representation of the contact scenario, facilitating a more focused wear analysis. By applying the GW model, the proposed method enables a more direct assessment of the contact area, which is a key parameter in wear calculations.

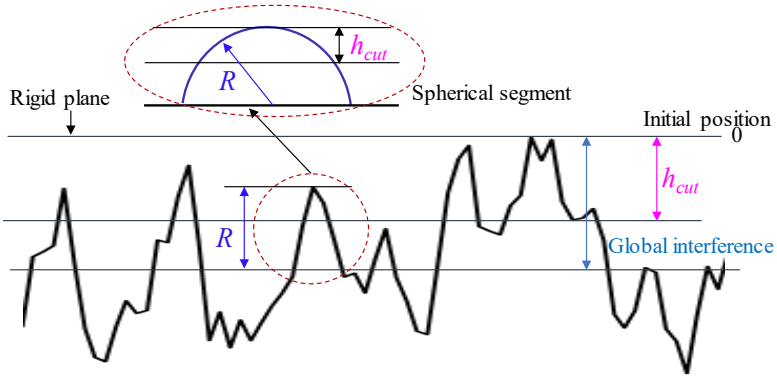

Figure 2. Schematic diagram of the two-dimensional contour of an equivalent rough surface truncated by a rigid plane.

The proposed conceptual model, as depicted in Figure 3, simplifies the complex wear process by treating the asperities as hemispheres. This geometric simplification allows for a more analytical approach to understanding and quantifying the wear behavior of the sheet metal. By considering the wear process as the sequential cutting of these hemispheres, the model provides a framework for estimating the volume of material removed due to wear, which is directly related to the depth and extent of the surface asperities.

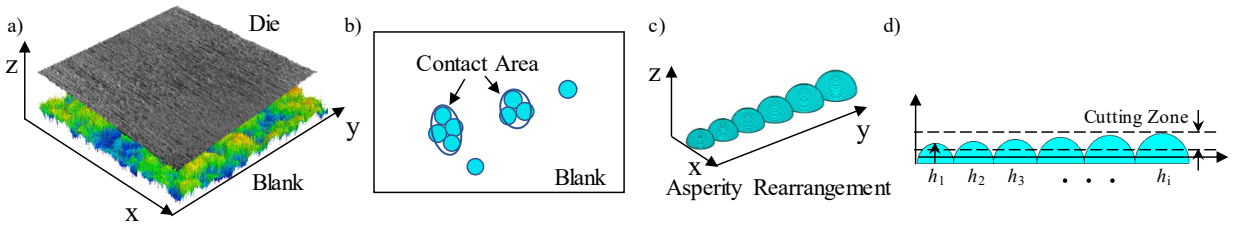

Figure 3. (**a**) Schematic representation of the contact zone on the surface of the metallic sheet material, (**b**) illustration of the wear-induced micro-protuberances on the surface of the steel substrate, (**c**) hypothesis regarding the micro-asperities present on the surface of the sheet metal, and (**d**) depiction of wear patterns on the micro-asperities of the surface.

This approach to modeling wear is particularly useful in hot stamping, in which the high temperatures and pressures can exacerbate the wear process. By quantifying the wear in terms of the removal of micro-asperities, the model can help in predicting the evolution of the sheet metal surface over the course of stamping.

From the GW model analysis, it is known that the micro-asperities on the surface of the sheet metal can be considered to be composed of hemispheres of different heights (R), as shown in Figure 3. Here, R represents the radius of the hemisphere corresponding to each micro-asperity. When the micro-asperity plane is cut by a horizontal plane, the total horizontal area composed of the cut-off bottom of the spheres is A_r. We use integration to represent the total volume of the cut-off spheres. First, assume that the radius of the base of the cut-off sphere is h, which is given as follows:

$$h = f(h_{\text{cut}}) \tag{4}$$

where $f(h_{\text{cut}})$ is the height distribution function of the surface micro-asperities, and h_{cut} (μm) is the height at which the micro-asperity has been cut.

Then, we analyze the number of micro-asperities at the cutting height h_{cut}, which is the number of micro-asperities per unit height. Combined with the real contact area A_r, the number of micro-asperities per unit height is expressed because A_r represents the total contact area of the micro-asperities at the height h_{cut}. The density of the micro-asperities can be expressed as the ratio of the number of micro-asperities per unit height to the real contact area. Therefore, the density of the micro-asperities at height h can be represented as follows:

$$\frac{A_r}{\pi[f(h)]^2} \tag{5}$$

where A_r (μm²) is the real contact area in square micrometers.

To calculate the total number of micro-asperities within a range of height h_{cut}, we need to sum the densities of micro-asperities at each height. Consequently, the total number of micro-asperities can be expressed as an integral of the density function over the following height range:

$$N = \int_0^{h_{\text{cut}}} \frac{A_r}{\pi[f(h)]^2} dh \tag{6}$$

Ultimately, the precise quantification of the wear volume for micro-asperities is achieved by defining the height of material removal for each micro-asperity as h_i. By

employing the principle of integration, the volumetric wear of micro-asperities at a specified cutting depth h_i is determined as follows:

$$dV_{Asperity} = \frac{\pi {h_i}^2}{3}(3f(h_i) - h_i)dh_i \tag{7}$$

where $\pi {h_i}^2$ (μm²) is the area of the cut micro-asperity with radius h_i in square micrometers.

When calculating the total volume of the cut spherical micro-asperity, we use the infinitesimal method to decompose the spherical cap into infinite micro-asperity volumes as follows:

$$V_{Total} = \int_0^{h_{\text{cut}}} dV_{Asperity} \tag{8}$$

Combining the micro-asperity density and micro-asperity volume, we merge the micro-asperity density N and the micro-asperity volume dV to obtain an expression for the total volume of the cut micro-asperity as follows:

$$V_{Total} = k\int_0^{h_{\text{cut}}} \frac{A_r}{\pi[f(h)]^2} \cdot \frac{\pi h^2}{3}(3f(h) - h)dh \tag{9}$$

where k is the wear coefficient of the sheet metal, a dimensionless parameter; A_r (mm²) is the real contact area during the wear process in square millimeters; $f(h)$ is the height distribution function of the surface micro-asperities in micrometers; and h (μm) is the height of the surface micro-asperities in micrometers.

3. Experiments

3.1. Parameters and Procedures

To simulate the friction conditions between high-temperature boron steel sheet metal and a water-cooled die during the hot stamping process, a custom-made differential temperature friction testing device was employed for the friction and wear experiments [35]. The experimental setup was meticulously designed to replicate the thermal gradients and pressures encountered during the hot stamping process. The parameters for these experiments, detailed in Table 1, were selected to encompass a range of conditions that would yield comprehensive data on the friction and wear behavior of the materials involved.

Table 1. Wear experiment parameters.

Condition	Parameter
Blank temperature (°C)	650, 700, 750
Hardness of pins (HRC)	50 ± 2
The diameter of the pin (mm)	3.5
Blank size (mm)	$69 \times 20 \times 1.4$
Sliding speed (mm/s)	4
Normal Load (N)	30, 50, 70
Time (s)	9

The friction pin is made of hot working die steel (AISI H13). By setting different load levels at various temperatures, the experiments aimed at simulating the pressure changes under different process conditions. According to the experimental requirements, the friction disk was heated, while the upper friction pin was cooled. A control system regulated the heating rate of the sheet metal. Figure 4a illustrates the set temperature histories of the steel plate and pin, and Figure 4b illustrates a schematic representation of the experimental apparatus utilized for the wear study.

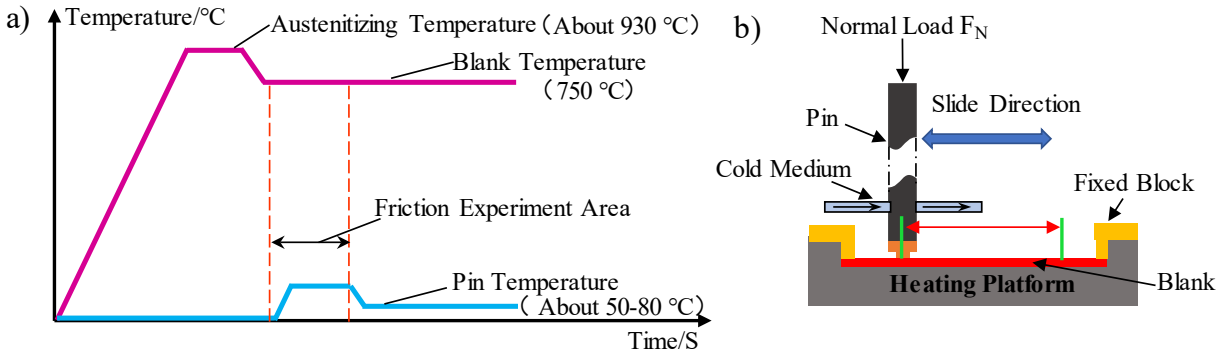

Figure 4. (**a**) Temperature variation curve between the plate and friction pin during the experimental process; (**b**) structural schematic diagram.

3.2. Wear Amount Analysis

At temperatures between 650 and 750 °C, the galvanized layer surface of advanced high-strength steels exhibits a complex phase composition; the main phases on the galvanized layer surface include δ-FeZn10, γ-ZnFe, α-FeZn, and α-FeZn [33,36], recognizing the significance of these phases in dictating wear behavior. Therefore, to more accurately analyze the theoretical wear amount, a 3D profilometer was used to calculate the volume wear amount based on the average profile of the wear track cross-section [37,38]. The results obtained were compared with those predicted by the model, providing a more reliable basis for validating the wear model.

In the field of tribology, the detailed characterization of wear tracks is crucial for understanding the wear mechanisms and optimizing the performance of materials under various loading conditions. Following the differential temperature sliding wear test, this study delves into the three-dimensional (3D) morphology analysis of the wear track on the surface of the sheet metal, a critical step in elucidating the wear behavior of the material.

Based on the differential temperature sliding wear test, a three-dimensional morphology analysis of the surface of the sheet metal wear track was conducted, with the average height of the wear track representing the wear height. A 3D profilometer was used to perform detailed measurements of the wear track morphology on the surface of the GA steel sheet. Different cross-sections were selected, and measurements were taken in the vertical direction of the sheet metal wear track to obtain two-dimensional morphology data of the wear track, as shown in Figure 5.

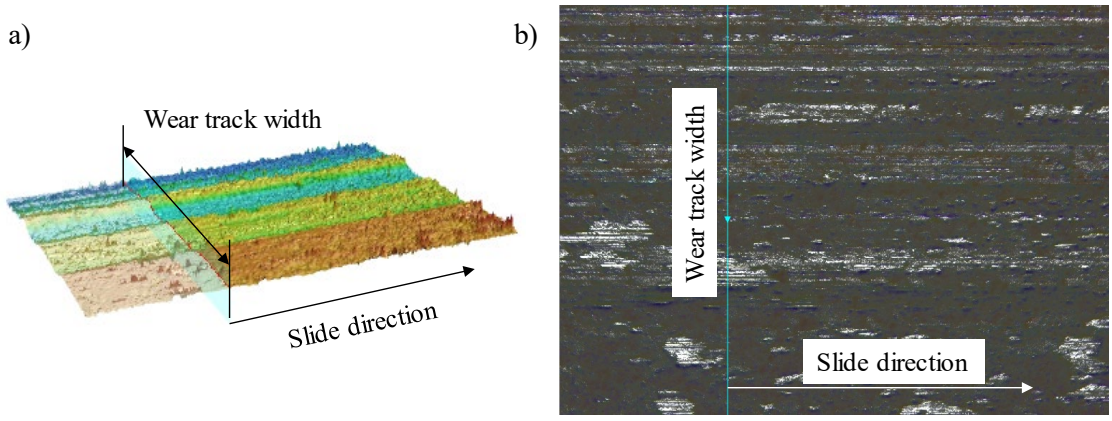

Figure 5. (**a**,**b**) Cutting of two-dimensional contour of surface grinding tracks on sheet metal.

Using the above method, in order to more comprehensively analyze the wear condition of the sheet metal, an analysis was conducted on the wear track width curve for each cross-sectional profile obtained from Figure 6. In conjunction with the distribution of fracture heights of micro-protuberances on the coating surface within the wear track, the

reference line (6 μm) and the regions of material loss were determined. By defining the two-dimensional morphology of the wear track cross-section, the reference line was set as the average reference line of micro-protuberances on the surface of the unworn area. Above the reference line is the adhesive wear portion, and the area below the reference line is the material loss area, as specifically shown in Figure 6. Figure 6 clearly displays the height variation of the sheet metal wear surface under 650 °C, 30 N. The area below the reference surface is denoted as Su. The average total area of material loss obtained from n profiles in the sheet metal wear region (Su_m) can be represented in the following manner:

$$Su_m = \sum_{p=1}^{n} Su_p / n \tag{10}$$

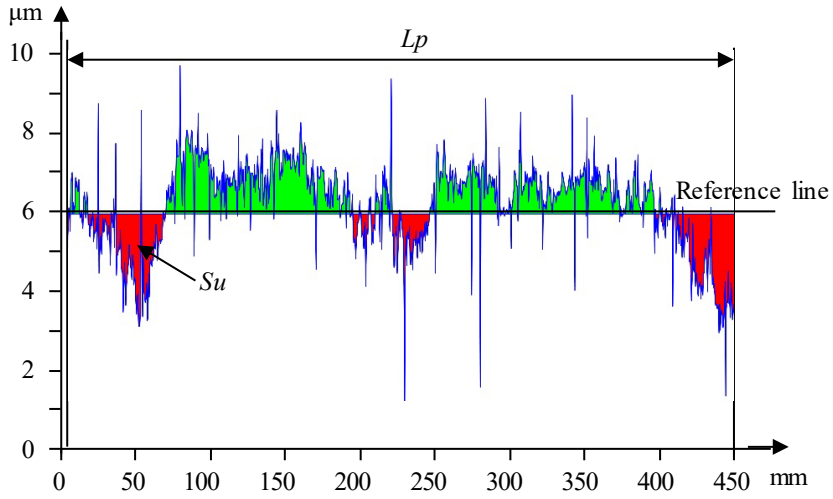

Figure 6. The cross-sectional profile of a worn surface at—650 °C, 30 N (green for transfer, red for loss).

Therefore, the wear volume Sv of the sheet metal can be expressed as follows:

$$Sv = Su_m \times Lp \tag{11}$$

where Su_m (μm^3) is the average of the total cross-sectional area loss of the sheet metal, Lp = 3.5 (mm) is the total length of the wear track, and n (n = 30) is the number of cross-sections.

In the quest to elucidate the wear behavior in hot stamping processes, a comprehensive experimental campaign was executed on multiple specimens, with each subjected to distinct conditions. The wear depth, a pivotal parameter, was meticulously quantified using a 3D profilometer, capturing the nuanced topographical changes across wear tracks. Morphological data were systematically gathered from varied segments of the wear paths, ensuring a representative analysis (Equation (11)). By applying a volume-averaging calculation formula to data extracted from 30 discrete wear track interfaces, this study derived the average wear volume, offering a robust metric for material loss. Figure 6 visually encapsulates the cross-sectional profile of a worn track.

4. Results and Discussion

In the context of advanced manufacturing processes, particularly hot stamping, the fidelity of wear prediction models is crucial for the reliability and efficiency of industrial applications. This study presents a critical comparative analysis of the actual wear measurements and the theoretical wear calculations for sheet materials subjected to hot stamping processes, as delineated in Figure 7, in which Ar = 1.638 mm^2 and k = 9.

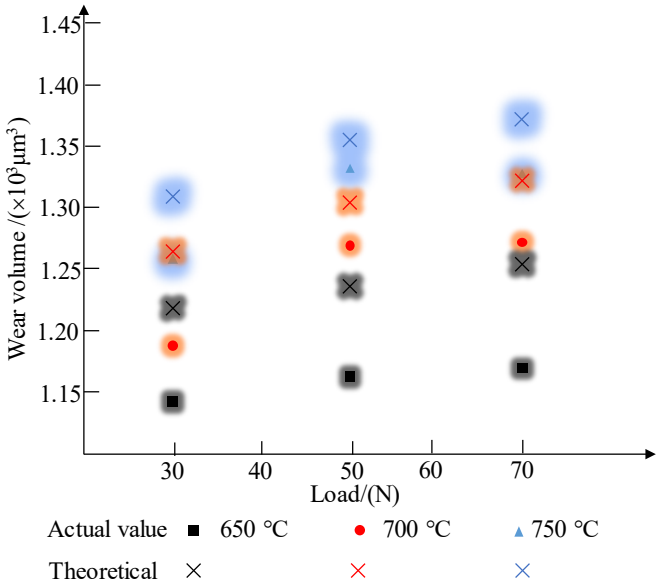

Figure 7. Comparison of actual and theoretical wear volumes.

In the context of advanced manufacturing processes, particularly hot stamping, the fidelity of wear prediction models is crucial for the reliability and efficiency of industrial applications. This study presents a critical comparative analysis of the actual wear measurements and the theoretical wear calculations for sheet materials subjected to hot stamping processes, as shown in Figure 7.

The initial findings underscore a notable alignment between the empirical data and theoretical predictions under low-load scenarios, with discrepancies well within tolerable limits. This congruence validates the model's applicability under less demanding conditions, providing a baseline for further investigation.

However, a discernible divergence emerges as the load intensifies, with the empirical wear measurements surpassing theoretical estimates, particularly at elevated load conditions. This deviation suggests that the theoretical model may not fully encapsulate the wear dynamics under more severe stress conditions.

The observed discrepancy at higher loads can be ascribed to several factors. The nonlinear material response under high stress, which is not fully captured by the current model, is a significant contributor. Additionally, wear mechanisms such as abrasive wear, induced by asperity interactions, and oxidative wear, accelerated by the high temperatures inherent to hot stamping, are likely to exacerbate material loss beyond the model's predictions.

Furthermore, experimental measurement errors, including those stemming from the precision of measurement instruments and the accuracy of the experimental setup, may introduce uncertainties that affect the comparative analysis.

To enhance the predictive accuracy of the model, future research must integrate a more nuanced understanding of these wear mechanisms and refine the theoretical framework accordingly. The incorporation of empirical data from a broader range of load conditions, alongside rigorous experimental methodologies, will be pivotal in achieving a more robust predictive model.

5. Conclusions

The methodology developed in this research accounts for the intricate interactions between the tooling and the material surface, particularly emphasizing the role of microprotuberances that are prevalent in the zinc layer of GA-UHSS. These micro-features, though small in scale, can significantly influence the overall wear behavior of the material when subjected to the high temperatures and pressures characteristic of hot stamping.

To substantiate the proposed contact model, experimental data were collected under controlled conditions at temperatures of 650 °C, 700 °C, and 750 °C, which are represen-

tative of the thermal environment in hot stamping operations. The model's predictive accuracy was evaluated under low-pressure conditions, demonstrating a commendable alignment with empirical measurements. By providing a more precise prediction of wear, the model can guide the adjustment of process parameters to mitigate unnecessary wear, thereby extending the service life of tools and enhancing the quality of the formed parts.

Author Contributions: Supervision H.Z.; methodology W.C.; writing—original draft preparation Y.P. All authors have read and agreed to the published version of the manuscript.

Funding: This research received no external funding.

Data Availability Statement: The original contributions presented in the study are included in the article, further inquiries can be directed to the corresponding author.

Conflicts of Interest: The authors declare no conflicts of interest.

References

1. Singh, J.; Khan, M.S.; Oliveira, J.P.; Arora, K.S. Brazing of high-strength steels: Recent developments and challenges. *J. Manuf. Process.* **2024**, *115*, 289–309. [CrossRef]
2. Li, J.; Tong, C.; Zhang, R.; Shi, Z.; Lin, J. A data-informed review of scientific and technological developments and future trends in hot stamping. *Int. J. Lightweight Mater. Manuf.* **2024**, *7*, 327–343. [CrossRef]
3. Bruschi, S.; Ghiotti, A.; Simonetto, E. 3.08—Hot stamping of high strength-to-weight metal alloys. In *Comprehensive Materials Processing*, 2nd ed.; Hashmi, S., Ed.; Elsevier: Oxford, UK, 2024; pp. 181–208.
4. Güler, H.; Ertan, R.; Özcan, R. Investigation of the hot ductility of a high-strength boron steel. *Mater. Sci. Eng. A* **2014**, *608*, 90–94. [CrossRef]
5. Zhang, Y.; Qin, Y.; Chen, T.; Ji, C. Improvement of microstructure and mechanical properties of laser welded Al-Si coated 22MnB5 steel joints by austenitic element copper. *Mater. Today Commun.* **2024**, *39*, 108989. [CrossRef]
6. Guo, N.; Zhang, X.; Hou, Z.; Wang, W.; Yang, D.; Min, J.; Ming, P.; Zhang, C. Hot stamping of ultra-thin stainless steel sheets for bipolar plates. *J. Mater. Process. Technol.* **2023**, *317*, 117987. [CrossRef]
7. Chantzis, D.; Tracy, M.; Liu, H.; Politis, D.J.; Fu, M.W.; Wang, L. Design optimization of hot stamping tooling produced by additive manufacturing. *Addit. Manuf.* **2023**, *74*, 103728. [CrossRef]
8. Hirtler, M.; Ünsal, I.; Buhl, J.; Bambach, M. Investigation of quench hardening behavior of directed energy deposited 22MnB5 steel for local reinforcement of hot stamping parts. *CIRP J. Manuf. Sci. Technol.* **2022**, *39*, 223–231. [CrossRef]
9. Wiklund, D.; Wihlborg, A.; Rosén, B.-G. Evaluation of surface topography parameters for friction prediction in stamping. *Wear* **2004**, *257*, 1296–1300. [CrossRef]
10. Billur, E. Hot stamping of ultra high-strength steels. In *From a Technological and Business Perspective*; Springer: Cham, Switzerland, 2019.
11. Ghiotti, A.; Bruschi, S.; Sgarabotto, F.; Bariani, P. Tribological performances of Zn-based coating in direct hot stamping. *Tribol. Int.* **2014**, *78*, 142–151. [CrossRef]
12. Ghiotti, A.; Bruschi, S.; Medea, F. Comparison of tribological and wear performances of AlSi and Zn coatings in hot stamping of boron steel sheets. *Wear* **2015**, *332*, 810–821. [CrossRef]
13. Hardell, J.; Prakash, B. High-temperature friction and wear behaviour of different tool steels during sliding against Al-Si-coated high-strength steel. *Tribol. Int.* **2008**, *41*, 663–671. [CrossRef]
14. Pelcastre, L.; Hardell, J.; Prakash, B. Tribological behaviour of Zn coated UHSS sliding against hot-work tool steel at high temperatures. *Wear* **2017**, *376*, 423–432. [CrossRef]
15. Kondratiuk, J.; Kuhn, P. Tribological investigation on friction and wear behaviour of coatings for hot sheet metal forming. *Wear* **2011**, *270*, 839–849. [CrossRef]
16. Schwingenschlögl, P.; Merklein, M. Characterization of tribological conditions within direct hot stamping. *J. Mater. Process. Technol.* **2020**, *278*, 116535. [CrossRef]
17. Wang, W.; Wang, K.; Zhao, Y.; Hua, M.; Wei, X. A study on galling initiation in friction coupling stretch bending with advanced high strength hot-dip galvanized sheet. *Wear* **2015**, *328–329*, 286–294. [CrossRef]
18. Zhou, L.; Gao, K.; Zheng, X.; Wang, W.; Wei, X.; Hua, M. Developing of galling during the forming and its improvement by physical vapour depositing. *Surf. Eng.* **2017**, *34*, 493–503. [CrossRef]
19. Gao, H.; Zhao, L.; Li, L.; Wu, S.; Lin, Z.; Wang, Q. Effect of Wear-Induced Surface Deformation on Stick-Slip Friction of Galvanized Automotive Steels. *Langmuir ACS J. Surf. Colloids* **2022**, *38*, 11459–11467. [CrossRef] [PubMed]
20. Zhuang, W.; Xie, D.; Chen, Y. Experimental investigation of the effect of the material damage induced in sheet metal forming process on the service performance of 22MnB5 steel. *Chin. J. Mech. Eng.* **2016**, *29*, 747–755. [CrossRef]
21. Zhuang, W.; Wang, P.; Xie, D.; Shi, H. Experimental study and a damage model approach to determine the effect of hot forming deformation on the service performance of 22MnB5 steel. *J. Manuf. Process.* **2019**, *47*, 10–21. [CrossRef]

22. Venema, J.; Matthews, D.T.A.; Hazrati, J.; Wörmann, J.; van den Boogaard, A.H. Friction and wear mechanisms during hot stamping of AlSi coated press hardening steel. *Wear* **2017**, *380*, 137–145. [CrossRef]
23. Yu, Z.Q.; Hou, Y.K.; Li, S.H.; Lin, Z.Q.; Zhang, W.G. Surface damage behavior of galvanized steel sheets in forming process under tension-bending. *Int. J. Mod. Phys. B* **2010**, *24*, 5877–5884. [CrossRef]
24. Archard, J.F.; Hirst, W. The wear of metals under unlubricated conditions. *Proc. R. Soc. London. Ser. A. Math. Phys. Sci.* **1956**, *236*, 397–410.
25. Hol, J.; Alfaro, M.; Rooij, M.; Meinders, T.; Felder, E.; Montmitonnet, P. Multiscale friction modeling for sheet metal forming. In Proceedings of the 4th International Conference on Tribology in Manufacturing Processes, ICTMP 2010, Nice, France, 13–15 June 2010.
26. Shisode, M.; Hazrati, J.; Mishra, T.; De Rooij, M.; Ton, V.D.B. Multi-Scale Contact Modeling of Coated Steels for Sheet Metal Forming Applications. *Key Eng. Mater.* **2018**, *767*, 223–231. [CrossRef]
27. Venema, J. Tribological Interactions and Modelling of Friction in Hot Stamping. Ph.D. Thesis, University of Twente, Enschede, The Netherlands, 2019.
28. Abspoel, M.; Neelis, B.M.; van Liempt, P. Constitutive behaviour under hot stamping conditions. *J. Mater. Process. Technol.* **2016**, *228*, 34–42. [CrossRef]
29. Kim, S.I.; Her, J.U.; Jang, Y.C.; Lee, Y. Experimental and finite element analysis for fracture of coating layer of galvannealed steel sheet. *Trans. Nonferrous Met. Soc. China* **2011**, *21*, s111–s116. [CrossRef]
30. Kondratiuk, J.; Kuhn, P.; Labrenz, E.; Bischoff, C. Zinc coatings for hot sheet metal forming: Comparison of phase evolution and microstructure during heat treatment. *Surf. Coat. Technol.* **2011**, *205*, 4141–4153. [CrossRef]
31. Han, K.; Lee, I.; Ohnuma, I.; Okuda, K.; Kainuma, R. Micro-Vickers Hardness of Intermetallic Compounds in the Zn-rich Portion of Zn-Fe Binary System. *ISIJ Int.* **2018**, *58*, 1578–1583. [CrossRef]
32. Han, K.; Ohnuma, I.; Okuda, K.; Kainuma, R. Experimental determination of phase diagram in the Zn-Fe binary system. *J. Alloys Compd.* **2018**, *737*, 490–504. [CrossRef]
33. Marder, A.R. The metallurgy of zinc-coated steel. *Prog. Mater. Sci.* **2000**, *45*, 191–271. [CrossRef]
34. Greenwood, J.A.; Williamson, J.B.P.P. Contact of nominally flat surfaces. *Proc. R. Soc. Lond.* **1966**, *295*, 300–319.
35. Chen, W.; Peng, Y.; Wang, Y.; Cao, P.; Zhu, Y.; Guo, Y. Research on high-temperature friction and wear performances of Stellite 12 laser cladding layer against coated boron steels. *Wear* **2023**, *520–521*, 204665. [CrossRef]
36. Su, X.; Tang, N.Y.; Toguri, J.M. Thermodynamic evaluation of the Fe–Zn system. *J. Alloys Compd.* **2001**, *325*, 129–136. [CrossRef]
37. Roux, S.L.; Boher, C.; Penazzi, L.; Dessain, C.; Tavernier, B. A methodology and new criteria to quantify the adhesive and abrasive wear damage on a die radius using white light profilometry. *Tribol. Int.* **2012**, *52*, 40–49. [CrossRef]
38. Pawlus, P.; Reizer, R. Profilometric measurements of wear scars: A review. *Wear* **2023**, *534–535*, 205150. [CrossRef]